Contributed paper

OPTO-ELECTRONICS REVIEW **11**(4), 327–337 (2003)

Fingerprint identification by using artificial neural network with optical wavelet preprocessing

M. ANTOWIAK and K. CHAŁASIŃSKA-MACUKOW*

Division of Information Optics, Institute of Geophysics, Faculty of Physics, Warsaw University, 7 Pasteura Str., 02-093 Warsaw, Poland

The advantages of optical wavelet transform used as a preprocessor for an artificial neural network are investigated. We show by digital simulation that this set-up can successfully identify and discriminate complex biometric images, such as fingerprints. The achieved capabilities include limited shift-, rotation-, scale- and intensity-invariance. We also show that the edges-enhancement filter, applied before the wavelet transform, significantly improves abilities of the system.

Keywords: optical fingerprint identification, biometrics, artificial neural network, optical wavelet transform.

1. Introduction

Biometrics is formed from the person's selected unique physical attributes which may be applied for the purpose of automated personal identification [1]. Typically, biometrics are based on features such as fingerprints, geometry of hand and vein patterns, iris or retinal patterns, image of a face, and characteristic features of the person's voice. The inherent feature of biometric data is its great complexity. Essential in this kind of images is high spatial-frequency details. Moreover, the differences among diverse classes of patterns are small which requires high discrimination capability of the system.

This paper discusses the capabilities of the hybrid system based on the optical wavelet preprocessor (OWP) and electronic artificial neural network (ANN) applied to fingerprints identification. Most digital processing methods for fingerprint identification are based on the extraction of minutiae, which are the most unique fingerprint features and they are defined as the fingerprint ridge endings and bifurcations [2]. The advantage of using optical approach, i.e., optical correlators [3–6] or artificial neural networks, instead of minutiae analysis is that a global operation on the images is less sensitive to local distortions that typically occur during the fingerprint reading procedure.

The aim of simulations presented here is to show that the wavelet preprocessor can improve the ability of an ANN to identify and discriminate the highly complex data such as fingerprints. This research is inspired by the results obtained by the Japanese team of Hirokawa, Itoh, and Ichioka [7]. They proposed multichannel hybrid system for character recognition based on neural networks architecture with multiwavelet transforms as a preprocessor. This system has in certain range invariance against rotation-, shift-, intensity- and scale- changes [8]. The achieved level of tolerance should provide satisfactory performance of the system working with the real-life distorted data. Special focus is given on the advantages provided by the preprocessing extracting features that are most important to the process of pattern identification.

The results shown here are achievable using discussed set-up with various techniques of preprocessing and ANN learning. The drawbacks and advantages of the examined system are investigated as well as the prospective directions of development.

2. ANN with optical wavelet preprocessor

A general scheme of presented recognition system is shown in Fig. 1. This system is a modification of the multichannel hybrid set-up described in Ref. 7. In this paper one-channel set-up with only one neural network and one wavelet transformed image is examined. Main core consists of an electronic ANN module and optical wavelet preprocessor based on VanderLugt correlator [9] (Fig. 2).

2.1. Optical wavelet preprocessor based on VanderLugt correlator

The value of optical wavelet transform (OWT) for the given parameters can be calculated as the cross-correlation function of a signal and particular wavelet function [10]. Using the optical correlator is natural and effective method to obtain it [11]. In the spectrum plane of correlator we obtain product of the Fourier spectrum of input image $s(x,y)$ and the conjugate Fourier transform (FT) of the wavelet

*e-mail: kmacukow@mimuw.edu.pl

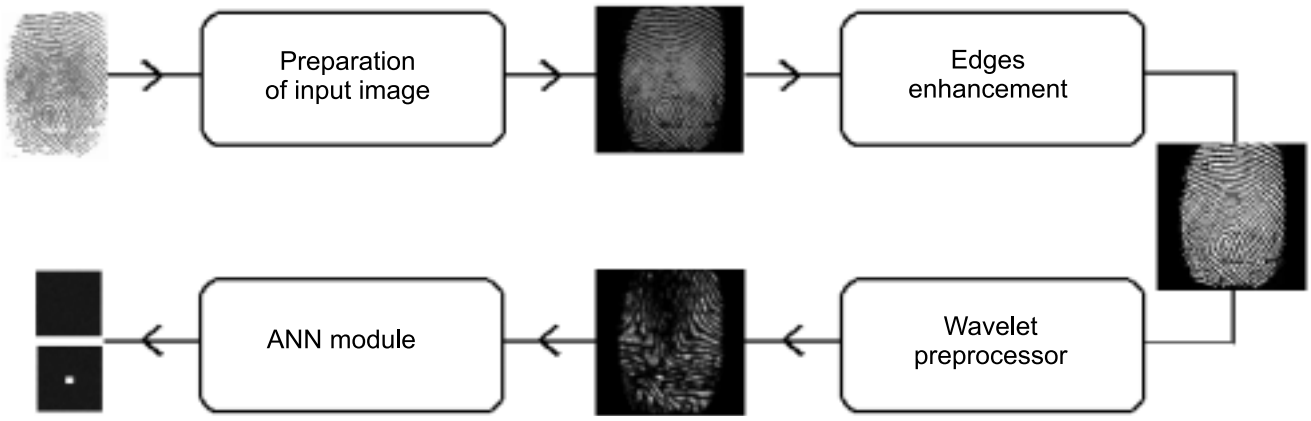

Fig. 1. Flow chart of the recognition system.

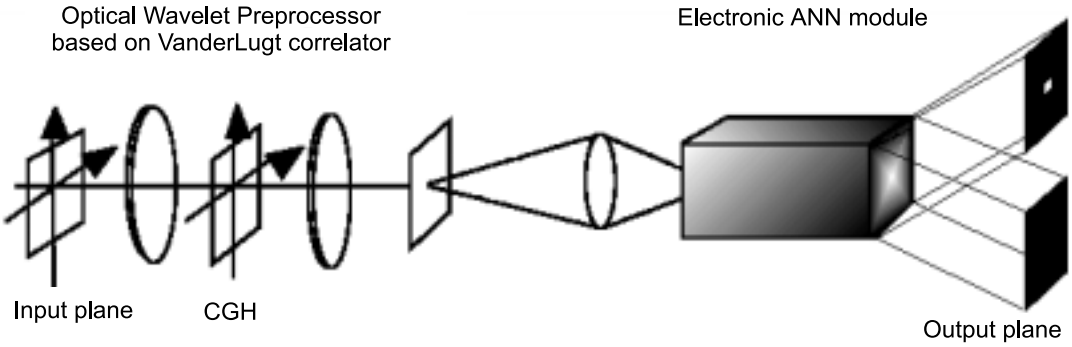

Fig. 2. Electronic ANN module with Optical Wavelet Preprocessor based on VanderLugt correlator.

$h(x,y)$ (which is normally coded on the CGH) which is equivalent to the Fourier Transform of the $w_s(.)$. So, the basic formula takes the form

$$FT[w_S(a,b,c,d;x,y)] = \sqrt{ab}H^*(a\nu_1, b\nu_2)S(\nu_1,\nu_2), \quad (1)$$

where (ν_1,ν_2) are the coordinates in the Fourier plane, $H(\nu_1,\nu_2) = FT[h(x,y)]$, $S(\nu_1,\nu_2) = FT[s(x,y)]$, and a, b, c, d are the parameters of the wavelet dauther, respectively. Next, by calculating the inverse Fourier transform, the wavelet transform $w_s(.)$ of the input signal is obtained.

The wavelet processor is a classical VanderLugt correlator with a computer generated hologram (CGH) placed in the Fourier plane [11]. Because the DC component of the wavelet spectrum is equal to zero, coding the spectra on the CGH requires only small number of quantization levels, and therefore the quantization related error is less than 1% [7]. The optical wavelet transform can be performed with many other set-ups [10–15], but CGH offers superior flexibility. It does not only provide an easy way to change the wavelet, its scale or shape, but also allows parallel realization of multiple wavelet transforms. Depending on the required number of wavelets, spatially separated images of wavelet transforms can be obtained by adding appropriate spectra.

In this experiment, the obtained OWT images were down-sampled according to the scale of wavelet. The larger scales of wavelets correspond to lower spatial-frequencies and therefore the sampling is preformed with the bigger interval. For small wavelet scales the sampling is more denser. This operation reduces the redundancy in the object in order to improve the generalization ability of ANN.

2.2. Electronic ANN module

The architecture of ANN used in the simulated system is based on the FELSI (feed forward model with local space-invariant interconnections) model introduced and developed by the group of professor Ichioka [7,8]. The network, as illustrated in Fig. 3, consists of layers of clusters. Each cluster is composed of 64×64 neural units. The units in the input layer have linear activation function, whereas units in all other layers have bipolar sigmoid activation function $\Psi(x)$

$$\psi(x) = \frac{1 - e^{-x}}{1 + e^{-x}}. \quad (2)$$

All the tested networks have two hidden layers, but number of clusters in these layers varies. The structure of a FELSI unit can be symbolically described as: 1-X-Y-2, which means that there is one cluster in the input layer, X clusters in the first hidden layer, Y clusters in the second hidden layer and two clusters in the output layer. For exam-

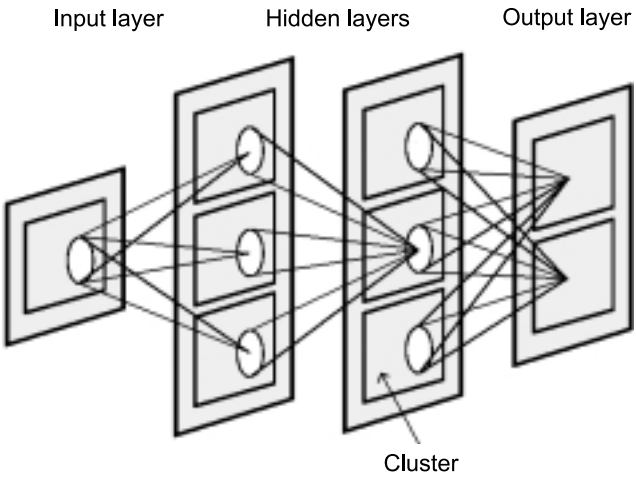

Fig. 3. Architecture of FELSI model (after Refs. 7 and 8).

ple, the network presented in Fig. 3 can be described as 1-3-3-2. In all experiments the size of weight matrices was 11×11 between the input and the first hidden layer and 21×21 between other layers. The formulas of backpropagation algorithm for the FELSI network can be found in Refs. 7–9.

2.2.1. Learning procedure of ANN

The samples of fingerprints were taken by the Internet from the database of Bologna University [16]. The size of samples was 90×128 pixels. Two fingerprints were chosen arbitrarily. Next, the negatives were taken and placed centrally in the black 128×128 scene. As a result the 128×128 black (zero pixel value) input scenes with white (pixel values in the [0,255] range) ridges are obtained [see Figs. 4(a) and 4(b)]. As the optional stage of preprocessing, the edges-enhancement filter presented in Fig. 5 was applied.

To provide comparability of the results, the same two fingerprints [Figs. 4(a) and 4(b)] were used as training patterns for all simulations. In the following sections they are referred to as 1_0 and 4_0, respectively.

Before the signal is fed to the ANN, the down-sampling is performed. In the experiment, the wavelet dilation parameters for both directions were $a = b$. The down-sampling interval is inversely proportional to the scale of the wavelet

$$w(x, y) = w_S(ax, ay). \tag{3}$$

Fig. 4. Training patterns used for all systems: (a) 1_0 and (b) 4_0.

–1	–1	–1
–1	–9	–1
–1	–1	–1

Fig. 5. Edges-enhancement filter.

After that, the image is centrally placed on the 64×64 black background and normalized within the range [–1,1].

The initial values of weights and biases are random. Contrary to Ref. 7, where initial values were "extremely small", the fastest and most certain convergence is achieved for initial weights randomly distributed in range $[-2.38/\sqrt{n}, 2.38/\sqrt{n}]$, where n is the fan-in of a unit (the number of units which are fed forward to this unit) [5 after 39]. The smaller initial values tend to make the learning process vulnerable to undesirable local minima.

In the process of supervised learning, the resilient backpropagation (RPROP) algorithm [17] and the batch update mode is applied. In each epoch, both training patterns are fed to the network with the corresponding pairs of target patterns in the output clusters. The parameters of RPROP are set to: $\Delta_{min} = 10^{-6}$, $\Delta_{max} = 10^{-1}$, $\eta^- = 0.5$, $\eta^+ = 1.2$. Δ_{max} is significantly smaller than normally used, in order to support the weight-decay effect and avoid too fast growth of weights. The decay term varied from 10^{-6} to 10^{-4}.

In most cases, the additional noise is introduced in the input plane. In such a situation, for every epoch, random uniformly distributed noise is generated and added to the training patterns. This modification of the learning algorithm, although improves the generalization ability, also significantly slows down the learning process and, in many cases, it does not allow the process to converge at the desired error level.

The learning error function is defined as

$$error = \frac{1}{CSXY} \sum_{c}^{C} \sum_{s}^{S} \sum_{x}^{X} \sum_{y}^{Y} \left| T_{c,s}(x, y) - O_{c,s}(x, y) \right|, \tag{4}$$

where (x,y) are the coordinates in a cluster, S is the number of training patterns, and C is the number of clusters in the output layer. In all experiments, $X = Y = 64$, $C = 2$, and $S = 2$.

The first step in the process of learning was to choose the desired value of error function. If the error is too high, the discrimination ability may be not satisfactory. On the other hand, the risk of overfitting causing the deterioration of the generalization ability, must be taken into account. To

find the proper level of an error, as the preliminary tests, the learning was stopped at different stages and the properties of the obtained networks were examined. As a result, the range $[2\times10^{-3}, 3\times10^{-3}]$ was found to give the best results. To compare, when all output units have the values exactly reverse to the target patterns, the error function equals 2. When only one unit has reverse value the error equals 1.2×10^{-4}.

Occasionally, even though the RPROP algorithm was used, the learning process was not able to escape an undesirable local minimum. In such a situation, the "jog of weights" method was applied [17]. It was observed that this technique was usually successful when the range of random changes was higher than 75% of weights value. Of course, when the first try did not bring the expected result, the operation could be repeated with the bigger range of changes. Regrettably, in many cases, especially when the high level of additional noise was used, this technique was not able to help the learning algorithm to avoid getting stuck in very broad minima. As a result, some networks described below have the learning error higher than recommended one.

2.2.2. Postprocessing of an output signal

The ANN is supposed to discriminate between two classes of patterns, so two clusters in the output layers are used. When the network is fed with a sample belonging to the class no. 1, it is expected to produce the "yes" pattern in the cluster no. 1 and the "no" pattern in the other cluster. When a sample from the class no. 2 is presented, the response should be inverse. The output signal corresponding to "yes" pattern is the 6×6 matrix of excited (+1 value) pixels on the background composed from pixels with –1 value [see Fig. 6(a)]. The "no" pattern is simply the background with the output of all pixels equal to –1 [see Fig. 6(b)].

Defining the "yes" pattern as a 6×6 matrix of pixels, rather than only one pixel output, brings two benefits. First, the learning process is more stable, what means that it is faster and less likely to get stuck in a local minimum. Second, the obtained output can be better interpreted. As it is explained below, it is crucial to understand properly the output signal and the analysis of its deformation greatly contributes to correct identification.

When the learning process had been successfully finished, the systems performance was tested. Different input patterns were fed to the system and the signal in the output clusters of the ANN was analysed.

Fig. 6. Output signal corresponding to (a) "yes" and (b) "no".

To describe quantitatively the output signal, the parameter Q was defined

$$Q = \begin{cases} \min\left(\dfrac{M_1}{M_2}, 10\right), & \text{if } M_1 > M_2 \text{ and } M_1 > 0.0208 \\ (-1)\min\left(\dfrac{M_2}{M_1}, 10\right), & \text{if } M_1 < M_2 \text{ and } M_2 > 0.0208, \\ 0, & \text{otherwise} \end{cases} \quad (5)$$

where M_1 and M_2 are obtained as follows. First, the central parts of the output signals are normalized into the [0,1] range. Then, convolution with the 6×6 square of value +1 is performed. Finally, the maximum values M_1 and M_2 in both products of convolution are found.

Modulus of Q informs how certain the discrimination is, while sign indicates which pattern has been identified (positive value means the answer "yes" in cluster no.1 – fingerprint no.1 is recognized, negative value means the opposite). In ideal case Q is infinite, hence the hard-clipping at the value of 10 (–10) is applied.

This algorithm of post-processing has numerous advantages:

- only centrally located output peaks are taken into account. This reduces the probability of a false,
- the square-like output patterns are more important than isolated excited pixels,
- small peaks are ignored. The threshold is supposed to eliminate false alarms caused by output noise related to the fact that the network's learning process was stopped with a learning error higher than zero.

In many cases, when in both clusters the maximum values are equal and the method proposed in Ref. 7 fails, it still gives proper answer. Two examples of proper identification in uncertain situation are presented in Fig 7. In the upper pair of clusters both maxima equal +1, but in Fig. 7(a) the maximum lays outside the detection field and therefore is ignored. In this pair, Fig. 7(b) is interpreted as "yes" and Fig. 7(a) as "no" and the input sample is properly identified. In the lower pair of clusters, although both maxima are equal and lay in the detection field, the output Fig. 7(c) contains square-like pattern whereas in Fig. 7(d) the maximal unit is separated. Here, cluster in Fig. 7(c) is read as "yes" and in Fig. 7(d) as "no". Of course, the comparison of both output clusters is crucial and, in other circumstances, pattern in Fig. 7(d) could also be interpreted as "yes". It is important to choose proper level of certainty of identification.

3. Testing pattern

We used two test patterns to evaluate the performance of system. First, testing set consisted of patterns obtained from the training patterns [see Figs. 4(a) and 4(b)] by vari-

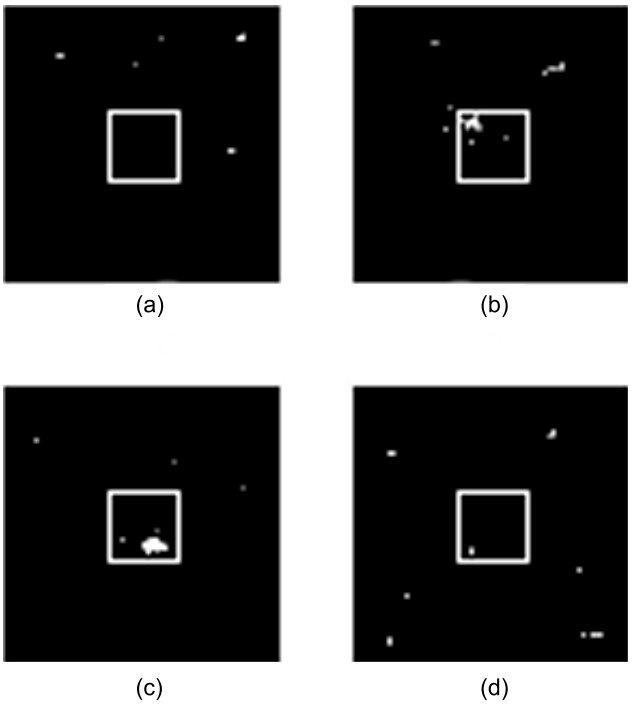

Fig. 7. Two pairs of output clusters. In the upper pair (a) is interpreted as "no" and (b) as "yes". In the lower pair (c) is interpreted as "yes" and (d) as "no". White square limits the field of

This test was supposed to check the "real-life" performance of the system. Every print of a given finger is the result of all possible distortions. In many cases the degree of deformation is much higher than in samples from the first group of tests. For example, the intensity distortion of the images (b) and (c) in Fig. 11 is evidently more severe than in Fig. 8(d). It is also significant that these samples often contain only a fragment of a training fingerprint [e.g., Fig. 10(g)] or even a different part of a finger. In such cases, the system cannot be expected to be able to give proper answer. It seems that the only solution is to collect the fingerprints more accurately. Since the influence of a distinct deformation cannot be measured or controlled, it is impossible to precisely evaluate the level of similarity between the training pattern and a given testing sample. Hence, only qualitative analysis can be performed.

4. Results of recognition – digital simulation

The procedure of numerical simulations explained above, in some cases with minor adjustments, has been applied to examine the performance of various configurations of the described system.

Fig. 8. Examples of deformations: (a) shift, (b) rotation, (c) scaling, (d) intensity change, and (e) occlusion. The edges-enhancement filter was applied after deformation.

ous types of deformation such as shift, rotation, scaling, irregular intensity changes, occlusion, "pinch" and "punch" operation. Figures 8 and 9 present some examples of these deformations. Since the main objective of this research was to check whether the examined system could be applied to identify the real-life distorted fingerprints, the invariance requirements should match a probable distortion caused by the inevitable inaccuracies of the fingerprint acquirement process. Accordingly, the required range of tolerance was: for rotation – 10°, scale 5%, shift – 10% of the input area, "pinch" and "punch" – 10%.

The "pinch" and "punch" effects are offered by the Paint Shop Pro 6 application and closely simulate real deformations (Fig. 9).

The second testing set enclosed the "real life" data which contained the different prints of the fingers used as training patterns. For both training fingerprints seven other samples were used (Figs. 10 and 11).

4.1. ANN without preprocessing

First, as a starting point, we examined the capabilities of the system without any preprocessing. This means that patterns 1_0 and 4_0 (Fig. 4) were directly fed to the ANN

Fig. 9. "Pinch" and "punch" deformations, (a) pinch – degree 15, (b) original image, (c) punch – degree 15. Deformations were made with Paint Shop Pro 6. The edge-enhancement filter was applied after deformation.

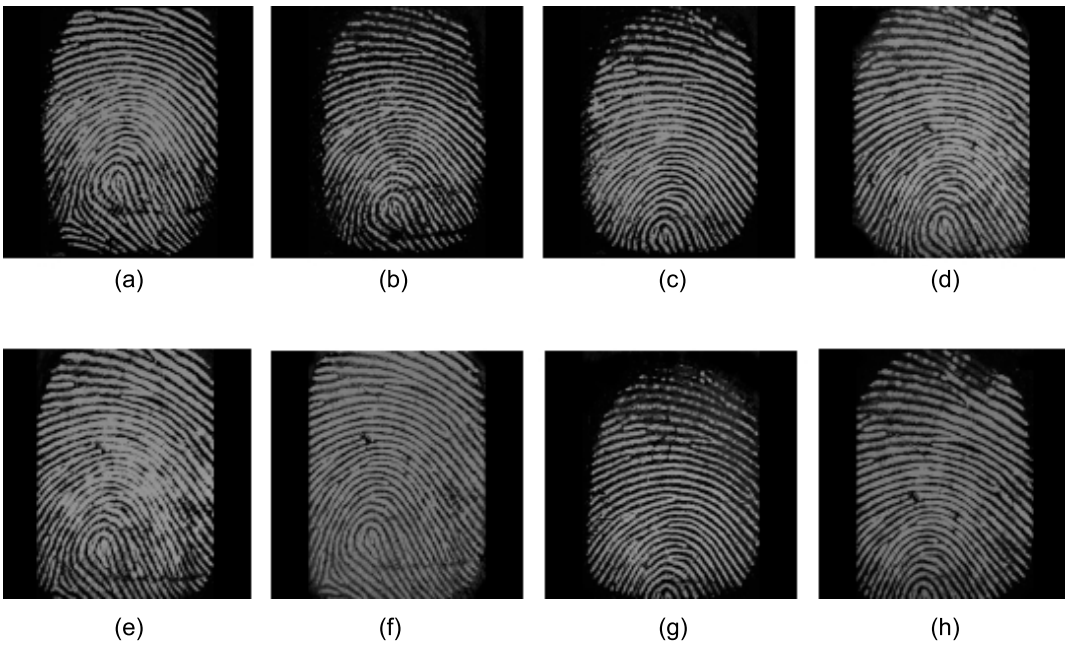

Fig. 10. Different prints of the finger no. 1. (a) training pattern 1_0 and (b)–(h) testing patterns.

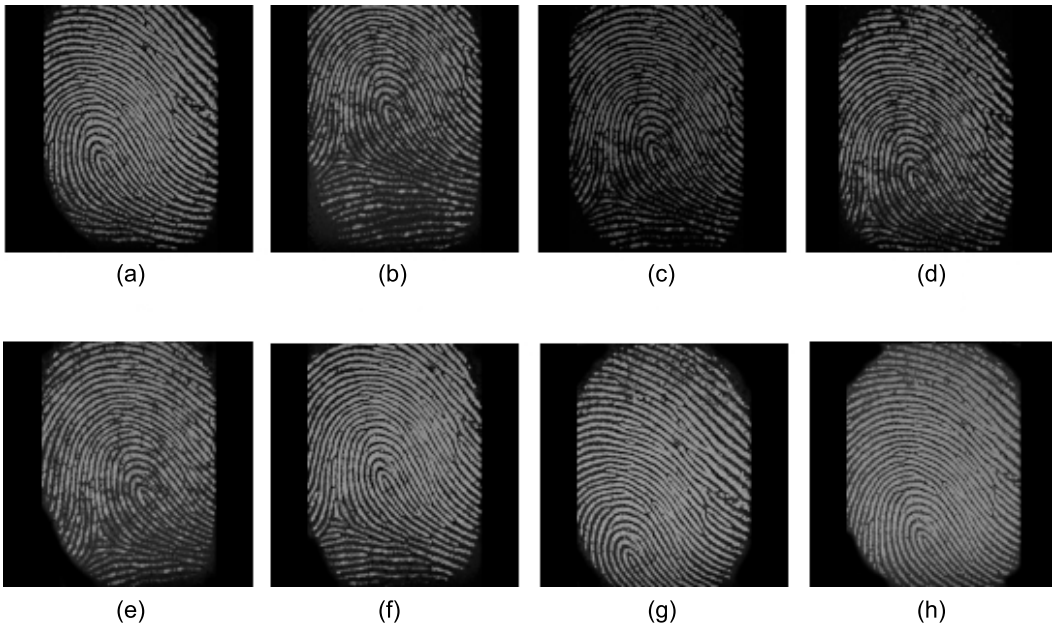

Fig. 11. Different prints of the finger no. 4: (a) training pattern 4_0 and (b)–(h) testing patterns.

module. A variety of learning parameters was used to obtain the best possible results. Two configurations of the FELSI unit: 1-3-3-2 and 1-4-4-2 have been tested. The smaller network proved to give better results, especially when noise was added. Performance of the set-up with 1-3-3-2 FELSI, noise range [–0.5,0.5] and learning error equal to 3.0×10^{-3} is presented in Table 1.

These numbers show that, although the system is shift invariant, it does not perform well when distorted images are presented. In the rotation range of 10° as much as 10% of samples was incorrectly identified and for another 12.5% the answer was "undecided". For intensity distortions only 23% of testing samples was identified correctly.

Table 1. Performance of the system with 1-3-3-2 FELSI, noise range [–0.5,0.5] and learning error equal to 3.0×10^{-3}.

Type of distortion	% of correct recognitions	% of wrong recognitions
Shift (13 pixels)	100.0	0.0
Rotation (1°–10°)	77.5	10.0
Intensity	23.0	0.0
Other – scale, pinch, punch, occlusion	20.0	5.0
"Rreal-life" samples	7.1	7.1

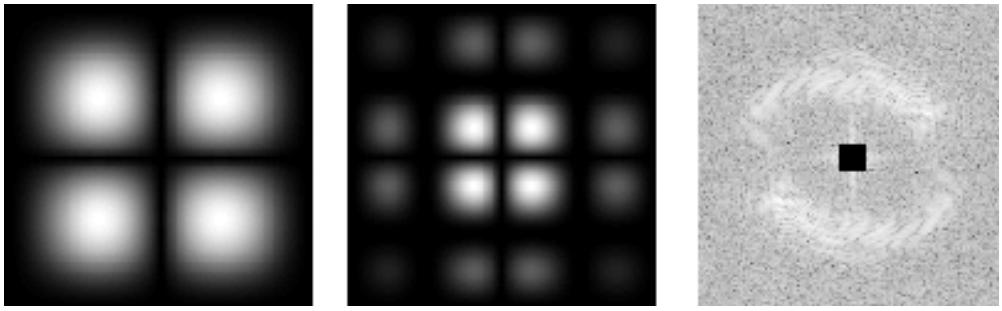

Fig. 12. Fourier spectra of: (a) Haar's wavelet of scale 2, (b) Haar's wavelet of scale 4, and (c) a fingerprint - logarithmic scale is used and the DC region is blocked to show higher frequencies.

In case of scaling, occlusion and "pinch" and "punch" the performance was even poorer. The second group of tests, conducted with different prints of the fingers used as training patterns, turned out to be more difficult. Only 1 out of 14 identifications was undoubtedly right and there was also one wrong recognition.

In this situation, preprocessing is proposed as the method to improve generalization and discrimination capability of the system.

4.2. ANN with edges-enhancement and wavelet transform in the preprocessing stage

The goal of this section is to find the configuration of the tested system that could provide good generalization ability and sufficient discrimination capability at the same time.

The idea of feature extraction is based on the reduction of information content to the required minimum. So, the main task is to define which part of image is crucial and which should be omitted. In the case of fingerprints, the high frequency details, such as ridges, are essential and the selected method of preprocessing must be sensitive to this kind of information. We chose to use the Haar's wavelet of scale 2. This choice can be confirmed by the analysis of Fourier spectra. Figure 12(c) illustrates the spectrum of a typical fingerprint. It is visible that a significant part of information is carried by the band of high frequencies. Most probably, this is the information crucial to the recognition process. Obviously, a suitable wavelet should not eliminate this band of frequencies. Figures 12(a) and 12(b) present the Fourier spectra of Haar's wavelets. The Haar's wavelet of scale 2 appears to best fit the spectrum of a fingerprint.

An additional preprocessing operation, performed before the wavelet transform, is proposed. The most basic, intuitive idea of preprocessing is the edges-enhancement. As such, it does not extract any particular kind of features or details, but partially removes unwanted distortions in an analysed image. Therefore the image, before being transformed by the wavelet preprocessor, was filtered with proper edges-enhancement filter (Fig. 5). Figure 13 presents training patterns before and after the edges are enhanced. It is visible that the edges-enhancement filter successfully recovers sharp ridges in the previously blurry areas. This effect can be clearly observed in the central region of pattern in Fig. 13(a).

All tests presented below have been performed with the Haar's wavelet of scale 2 coded in the wavelet preprocessor. For all samples the edges-enhancement filter was first applied. This means that samples in Fig. 4 have been filtered with the filter presented in Fig. 5 and then the wavelet transform was performed. Such preprocessed images were fed to the FELSI unit as the training patterns.

First, the influence of FELSI size on the systems' performance was examined. Two networks had been prepared: 1-3-3-2 and 1-4-4-2. In the learning process no additional noise was used. The decay parameter was set to 10^{-4}. In both cases the learning error was equal to 2×10^{-3}. Tables 2 and 3 illustrate the performance of both systems.

Although the performance of both systems is much better than of the system using "raw" data, there are still some misidentifications. In all tests, the system with 1-3-3-2 FELSI behaved better than the larger network. It is known that the generalization ability strongly depends on

Fig. 13. Training patterns: (a) pattern 1_0, (b) pattern 1_0 with enhanced edges, (c) pattern 4_0, and (d) pattern 4_0 with enhanced edges.

Table 2. Performance of the system with preprocessing (edges enhancement and Haar 2), 1-3-3-2 FELSI, decay parameter 10^{-4} and learning error equal to 2.0×10^{-3}.

Type of distortion	% of correct recognitions	% of wrong recognitions
Shift (13 pixels)	100.0	0.0
Rotation (1°–10°)	90.0	0.0
Intensity	95.0	0.0

Table 3. Performance of the system with preprocessing (edges enhancement and Haar 2), 1-4-4-2 FELSI, decay parameter 10^{-4} and learning error equal to 2.0×10^{-3}.

Type of distortion	% of correct recognitions	% of wrong recognitions
Shift (13 pixels)	100.0	0.0
Rotation (1°–10°)	75.0	2.5
Intensity	65.0	0.0

the number of free parameters in the neural network. Apparently, the 1-4-4-2 FELSI suffers from the excessive number of clusters in hidden layers. Thus, in following simulations the 1-3-3-2 network was used.

Let us to concentrate on the meaning of random noise added in the input layer during the process of learning. To analyse this topic more precisely, three identical systems were used. All had the 1-3-3-2 FELSI unit, all used edges-enhancement and Haar's wavelet of scale 2 in the preprocessor and for all Weight Decay with parameter 10^{-5} was employed. The only difference was the range of noise, which was [–0.25, 0.25], [–0.5, 0.5] and [–0.75, 0.75]. For the higher values of noise, the learning process did not properly converge. The performance of these systems is presented in Table 4.

These numbers clearly show that good tolerance for artificially distorted samples does not necessarily guarantee satisfactory performance when strongly deformed images are used.

While for controlled deformations the increased noise range provides better generalization ability, in case of the "real-life" its impact is more complex. The effectiveness of recognition is at 36% when the noise is in the range [–0.25, 0.25], reaches 50% for [–0.5, 0.5] noise-range and falls to 29% when noise is increased to [–0.75, 0.75]. The only benefit from the higher learning noise is elimination of false identifications. A similar effect was reported in Ref. 7.

The analysis of these results indicates that the [–0.5, 0.5] noise-range is the optimal trade-off between computational time and system's performance. Figure 14 gives the detailed information about identification of each testing sample. In virtually all cases the recognition is extremely sure. In Fig 14(c), all three "undecided" answers are for the occluded samples. This is acceptable since, in its nature, the neural network sees the input patterns as a whole, rather than concentrate on particular details. Apparently, some

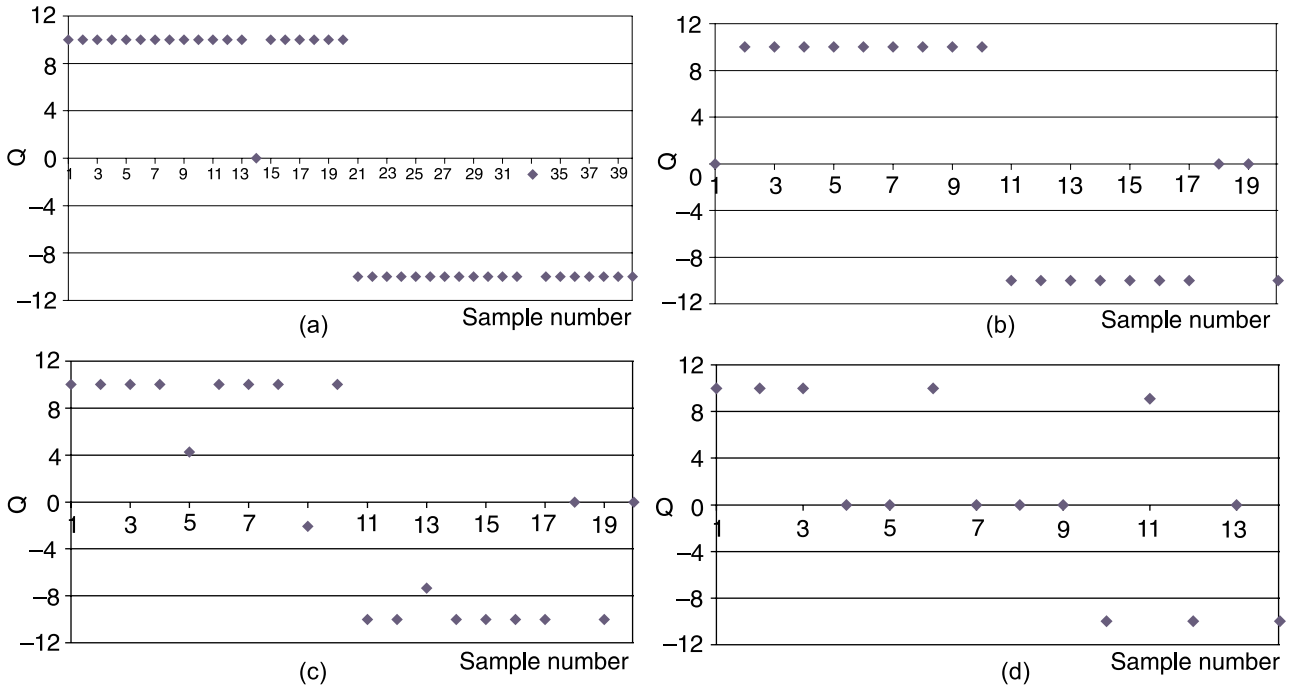

Fig. 14. System with preprocessing (edges enhancement and Haar 2). Test of the tolerance of a system with 1-3-3-2 FELSI and [–0.5, 0.5] noise range against: (a) rotation, (b) intensity distortions, (c) other deformations, and (d) real-life samples. In each chart the first half of points corresponds with the training pattern 1_0 and for them positive value of the parameter Q is expected. The second half of points corresponds with the training pattern 4_0 and negative value of the parameter Q is expected.

Table 4. Performance of the systems with preprocessing (edges enhancement and Haar 2), 1-3-3-2 FELSI, decay parameter 10^{-5}, learning error equal to 2.0×10^{-3} and various noise ranges.

	% of correct recognitions/% of wrong recognitions		
Type of distortion	[–0.25,0.25] noise range	[–0.5,0.5] noise range	[–0.75,0.75] noise range
Shift (13 pixels)	100.0/0.0	100.0/0.0	100.0/0.0
Rotation (1°–10°)	82.5/0.0	95.0/0.0	95.0/0.0
Intensity	70.0/0.0	85.0/0.0	80.0/0.0
Other – scale, pinch, punch, occlusion	75.0/0.0	85.0/0.0	85.0/0.0
"Real-life" samples	35.7/14.3	50.0/7.1	28.6/0.0

part of crucial information has been destroyed and, consequently, the recognition was impossible.

In the systems presented above, both edges-enhancement and wavelet transform were used in the preprocessing stage. This combined method of preprocessing gives good results, so it is worth investigating how big the role of each preprocessing operation is.

4.3. ANN with only edges-enhancement in the preprocessing stage

In order to assess the influence of edges-enhancement, a system identical with the set-up tested above, but without the wavelet preprocessor, was examined (Table 5).

At first, these results may seem unexpectedly disappointing, but when the real meaning of the edges-enhancement operation is fully understood, this poor performance can be fully explained. The generalization capability of this system is extremely limited. The system does not respond to slightly distorted samples. This is most probably caused by overfitting. Although the learning process in this test was stopped significantly earlier than in previous tests, the network lost its ability to generalize. The learning could be stopped even earlier, but in such case the discrimination capability, which already is not satisfactory, would suffer. These problems are associated with the way in which the edges-enhancement filter changes the image. The filtered image practically does not contain pixels of medium intensity. The ridges, which normally have slightly blurred boundaries, become sharp. This procedure is in fact equal to enhancement of high-frequencies.

Table 5. Performance of the system with preprocessing (only edges enhancement), 1-3-3-2 FELSI, decay parameter 10^{-5}, learning error equal to 2.0×10–3 and [–0.5,0.5] noise range.

Type of distortion	% of correct recognitions	% of wrong recognitions
Shift (13 pixels)	100.0	0.0
Rotation (1°–10°)	0.0	0.0
Intensity	5.0	0.0
Other – scale, pinch, punch, occlusion	00.0	0.0
"Real-life" samples	21.4	28.6

Table 6. Performance of the system with preprocessing (only wavelet transform – Haar 2), 1-3-3-2 FELSI, decay parameter 10^{-5}, learning error equal to 2.0×10^{-3} and [–0.5,0.5] noise range.

Type of distortion	% of correct recognitions	% of wrong recognitions
Shift (13 pixels)	100.0	0.0
Rotation (1°–10°)	52.5	10.0
Intensity	20.0	0.0
Other – scale, pinch, punch, occlusion	30.0	0.0
"Real-life" samples	0.0	21.4

4.4. ANN with only wavelet transform in the preprocessing stage

As the final test, the same system but with wavelet preprocessor instead of edges-enhancement filter was examined (Table 6). The discrimination capability of this configuration is not sufficient to provide reliable identification of distorted samples, especially when rotation is considered. In case of other deformations, the network usually is not able to give answer.

This indicates low generalization ability. The low level of selectivity of the feature extraction process is the probable cause of this situation. It is visible that only the combined method of edges-enhancement and wavelet-based feature extraction gives satisfactory results. In hardware implementations of the preprocessor, both these operations can be simultaneously performed by the properly prepared filter.

5. Conclusions

In this paper, a system consisting of an optical wavelet preprocessor and an electronic artificial neural network module has been examined. The aim was to check whether such system could be successfully employed to identify and discriminate highly complex biometric images, such as fingerprints. The required capabilities included shift-, rotation-, scale- and intensity-invariance. The additional constrain was the limited size of the training set. In fact, only one print of each finger was used as a training pattern, which was a significant impediment for the learning process.

Since, as it is shown above, performance of ANN working on raw data is not satisfactory, the preprocessing based on edges-enhancement and wavelet transform is proposed to enhance the generalization ability. Behaviour of various versions of the described set-up is presented.

In the optimal configuration proposed in this paper, the edges-enhancement filter first improves the quality of an input image. Owing to this procedure, the ridges in a fingerprint are more distinct. Subsequently, the optical wavelet processor is employed. The Haa's wavelet of a certain scale is used to extract specific features of an image. In future research other types of wavelet functions may be successfully applied.

The recognition is performed by the artificial neural network with built-in position invariance. Proper choice of the learning method additionally provides rotation-, scale-, and intensity-invariance. To some extent also occluded images can be properly identified.

The modified resilient backpropagation algorithm, which proved to be a significant improvement over the previously implemented standard backpropagation with momentum, can be successfully used in the learning process. The techniques of additional noise in the input layer and weight decay, joined with proper architecture of the network, noticeably improve the capabilities of the system.

The presented results confirm the assumption that preprocessing based on feature extraction enhances the generalization ability of an artificial neural network. Moreover, the discrimination capability is also significantly improved. Table 7 summarizes the best results obtained with various configurations of the examined set-up when controlled deformations were tested.

Surprisingly low rates of recognitions for system using only wavelet processor are probably caused by the employed method of interpreting the output signals. Possibly, if some less demanding method had been used instead, both correct and wrong recognitions rate would have been higher. Nevertheless, as it can be seen in the case of the last system, it is achievable to attain a reasonably high rate of correct recognitions and, at the same time, significantly reduce the probability of misidentification. The system using both edges-enhancement and wavelet processor in the preprocessing stage, provides very high reliability and satisfactory percentage of successful recognitions. At present, the results for the "real-life" data are not as promising as for the artificially prepared samples.

In future, the system's performance can be further improved in several ways. First of all, the accuracy of the data acquisition can be improved. Moreover, the size of training set can be increased. As it has been already mentioned, in further research other types of wavelets, especially the Morlet's wavelet, should be tested. Another improvement can be achieved by using the potential of CGH and employing simultaneously more than one wavelet and several ANN units. Such parallel system could provide better recognition rate with "real life" data, owing to the approach based on various features of the input image.

Table 7. The best obtained results of the set-ups with various methods of preprocessing. Only the controlled distortions (intensity, rotation, scaling, occlusion, pinch, punch) are considered.

Method of preprocessing	% of correct recognitions	% of wrong recognitions
No preprocessing	50.00	6.25
Wavelet processor	6.25	3.75
Edges-enhancement filter	40.00	8.75
Edges-enhancement + wavelet processor	88.75	0.00

References

1. S. Prabhakar, S. Pankanti, and A.K. Jain, "Biometrics recognition: security and privacy concerns", *IEEE Security&Privacy Magazine* **1**, 33–42 (2003).
2. A. Ross, A. Jain, and J. Reisman, "A hybrid fingerprint matcher", *Pattern Recognition* **36**, 1661–1673 (2003).
3. J. Rodolfo, H. Rajbenbach, and J.P. Huignard, "Performance of a photorefractive joint transform correlator for fingerprint identification", *Optical Engineering* **34**, 1166–1171 (1995).
4. Y. Pétillot, L. Guibert, and J.L. de Bougrenet de la Tocnaye, "Fingerprint recognition using a partially rotation invariant composite filter in a FLC joint transform correlator", *Optics Communications* **126**, 213–219 (1996).
5. A. Stoianov, C. Soutar, and A. Graham, "High-speed fingerprint verification using an optical correlator", *Optical Engineering* **38**, 99–107 (1999).
6. K. Chałasińska-Macukow and R. Kotyński, "Correlation methods in optical encription and security", in *Perspetives in Modern Optics & Optical Instrumentation*, pp. 197–193, edited by J.J. Joseph and K. Singh, Anita Publications, New Dehli, 2002.
7. K. Hirokawa, K. Itoh, and Y. Ichioka, "Invariant pattern recognition using neural networks combined with optical wavelet preprocessor," *Optical Review* (Japan) **7**, 284–293 (2000).
8. W. Zhang, K. Itoh, J. Tanida, and Y. Ichioka, "Parallel distributed processing model with local space-invariant interconnections and its optical architecture", *Applied Optics* **29**, 4790–4797 (1990).
9. M. Antkowiak, "Application of optical wavelet transform as a preprocessor for the artificial neural network in biometrics", M.Sc. Thesis, Warsaw University, Warsaw 2002.
10. Y. Li and Y. Sheng, "Wavelets, optics, and pattern recognition", Chapter 3 in *Optical Pattern Recognition,* edited by F.T.S. Yu and S. Jutamulia, Cambridge University Press, Cambridge, 1998.
11. K. Hirokawa, K. Itoh, and Y. Ichioka, "Real-time optical wavelet-transform with positive and negative signals", *Optical Review* (Japan) **4**, 366–369 (1997).
12. Y. Sheng, D. Roberge and H. Szu, "Optical wavelet transform", *Optical Engineering* **31**, 1840–1845 (1992).
13. K. Hirokawa, K. Itoh, and Y. Ichioka, "Optical wavelet processor by holographic bipolar encoding and joint transform correlation", *Applied Optics* **36**, 1023–1026 (1997).
14. K. Hirokawa, K. Itoh, and Y. Ichioka, "Optical wavelet transform using an LCTV-based joint transform correlator", *SPIE's International Technical Group News Letter* **11**, 6–7 (2000).
15. D. Mendlovic and N. Konforti, "Optical realization of the wavelet transform for two-dimensional objects", *Applied Optics* **32**, 6542–6546 (1993).
16. University of Bologna, Biometrics System Lab. Database DB2_B made available as a part of the Fingerprint Verification Competition, http://bias.csr.unibo.it/fvc2000/Downloads/DB_B.zip
17. A. Cichocki and R. Unbehauen, "*Neural Networks for Optimisation and Signal Processing*", John Wiley & Sons, New York, 1993.

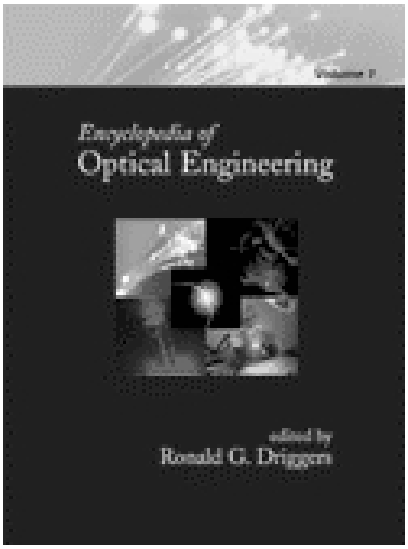

Encyclopedia of Optical Engineering
IN 3 VOLUMES

Edited by: Ronald Driggers

Purchase Options
List Price: $1,500.00
FREE ONLINE SUBSCRIPTION for one year with purchase of print edition!

Institutional orders for *Dekker Encyclopedias* cannot be placed through dekker.com. Subscriptions will be governed by an access/site license. Please contact sitelicenses@dekker.com
or call 1-800-228-1160 (USA, Canada & South America)
or 0041-61-260-63-00 (Europe, Far East, Middle East & Africa)
for ordering information.

Encyclopedia | Print Published: 09/01/2003 | Online Published: 09/01/2003
Hard Cover
2800 pages | Illustrated
ISBN: 0-8247-4258-3

Description

From astronomy to x-ray optics, this *Encyclopedia* contains more than 230 vivid entries examining the most intriguing technological advances and perspectives from distinguished professionals around the globe-selecting topics of utmost importance in areas including digital image enhancement, biological modeling, biomedical spectroscopy, and ocean optics for thorough coverage of recent applications in this continually expanding field.

Compiled by 300 of the most widely respected names in the electrooptic sciences, the *Encyclopedia* is destined to serve as the premiere guide in the field with nearly 2000 figures, 560 photographs, 260 tables, and 3800 equations.

Color graphics available online!
This one-of-a-kind reference delivers top-notch research on

- target detection
- image restoration
- fiber optic sources
- holography
- lens design
- classification and coding
- optical biopsy
- radiometry

Timely and dynamic, the *Encyclopedia* is an all-inclusive resource of the most significant and essential breakthroughs in photonics, imaging, and wireless communication.

